atmosphere

MDPI

Article

Can the Artificial Release of Fluorinated Gases Offset Global Cooling Due to Supervolcanic Eruptions?

Yangyang Xu [1,*], Nathanael P. Ribar [2], Jeffrey Sachnik [1], Gunnar W. Schade [1], Andrew John Lockley [3], Yi Ge Zhang [4], Pengfei Yu [5], Jianxin Hu [6] and Guus J. M. Velders [7,8]

1 Department of Atmospheric Sciences, Texas A&M University, College Station, TX 77843, USA
2 Department of Atmospheric Science, University of Wyoming, Laramie, WY 82071, USA
3 Independent Researcher, London, UK
4 Guangzhou Institute of Geochemistry, Chinese Academy of Sciences, Guangzhou 510640, China
5 Institute for Environmental and Climate Research, Jinan University, Guangzhou 511496, China
6 Department of Environmental Science, Peking University, Beijing 100871, China
7 National Institute for Public Health and the Environment (RIVM), Antonie van Leeuwenhoeklaan 9, 3721 MA Bilthoven, The Netherlands
8 Institute for Marine and Atmospheric Research Utrecht (IMAU), Utrecht University, Princetonplein 5, 3584 CC Utrecht, The Netherlands
* Correspondence: yangyang.xu@tamu.edu

Abstract: Large volcanic eruptions, such as the prehistoric Yellowstone eruption, induce abrupt global cooling—by some estimates at a rate of ~1 °C/year, lasting for more than a decade. An abrupt global cooling of several °C—even if only lasting a few years—would present immediate, drastic stress on biodiversity and food production. This cooling poses a global catastrophic risk to human society beyond the immediate and direct impact of eruptions. Using a simple climate model, this paper discusses the possibility of counteracting large volcanic cooling with the intentional release of greenhouse gases. Longer-lived compounds (e.g., CO_2 and CH_4) are unsuitable for this purpose, but selected fluorinated gases (F-gases), either individually or in combinations, could be released at gigaton scale to offset large volcanic cooling substantially. We identify candidate F-gases (e.g., C_4F_6 and CH_3F) and derive radiative and chemical properties of 'ideal' compounds matching specific cooling events. Geophysical constraints on manufacturing and stockpiling due to mineral availability are considered, alongside technical and economic implications based on present-day market assumptions. The effects and uncertainty due to atmospheric chemistry related to aerosol injection, F-gases release, and solar dimming are discussed in the context of large volcanic perturbation. The caveats and future steps using more complex chemistry–climate models are discussed. Despite the speculative nature of the magnitude and composition of F-gases, our conceptual analysis has implications for testing the possibility of mitigating certain global catastrophic cooling risks (e.g., nuclear winter, asteroid impact, and glacier transition) via intentional intervention.

Keywords: geoengineering; counter-geoengineering; simple climate model; supervolcanic eruptions; fluorinated gases

Citation: Xu, Y.; Ribar, N.P.; Sachnik, J.; Schade, G.W.; Lockley, A.J.; Zhang, Y.G.; Yu, P.; Hu, J.; Velders, G.J.M. Can the Artificial Release of Fluorinated Gases Offset Global Cooling Due to Supervolcanic Eruptions? *Atmosphere* **2024**, *15*, 1322. https://doi.org/10.3390/atmos15111322

Academic Editor: Meelis Zidikheri

Received: 25 September 2024
Revised: 27 October 2024
Accepted: 28 October 2024
Published: 2 November 2024

1. Introduction

Global warming brings ever-increasing risks and consequences [1], which are likely to become catastrophic if current emission pathways are not bent downward to net zero [2]. Alternatively, others have considered the risk of abrupt cooling due to natural or human causes (e.g., [3,4]). At least three drivers of global cooling are global catastrophic risks [5]: nuclear warfare [4,6], asteroid impacts [7,8], and large volcanic eruptions [3,9–12]. All involve injections of absorbing and/or reflective materials into the upper atmosphere, reducing tropospheric and surface insolation. Consequently, global average surface temperatures would drastically decline over a few years, gradually recovering as injected materials fall out.

Volcanic eruptions release sulfur dioxide (SO_2) from high-temperature magma [13,14]. Thermal plume buoyancy results in high-altitude deep convection well into the stratosphere [3,15]. In the stratosphere, SO_2 takes weeks to form sulfate aerosols, which scatter shortwave (SW) radiation back to space, leading to surface cooling. For example, the 1815 Mt. Tambora eruption on the island of Sumbawa, Indonesia, led to the subsequent "year without a summer" in 1816 [16]. Even larger "super" volcanic eruptions have the potential to produce a global cooling at a rate of 1 °C/year [3] (for reference, this is about 100-times faster than contemporary global warming, which on average is less than 0.01 °C/year since the industrial revolution).

Although temperature recovery after such global cooling events could be on the order of a decade, ecosystems and human society would face a major and potentially irreversible disruption. Agricultural yields—highly sensitive to changes in surface climate and solar insolation—would plunge worldwide [17–21]. As in 1815, this would likely result in the collapse of supply chains, civil disorder, and regional conflicts [22]. Enduring impacts of global cooling will exacerbate the immediate, near-term, and local effects (lavas, fires, and pyroclastic flow).

Volcanic eruptions also emit many other components beyond SO_2, from magma, as they rise toward the Earth's surface [23]. Water vapor plays a crucial role in driving explosive eruptions by increasing pressure within the magma. Carbon dioxide is released in significant quantities and contributes to the greenhouse effect, impacting the global climate [24], but over centuries to millennia, with a much lower warming rate. Other gases, such as hydrogen sulfide (H_2S), carbon monoxide (CO), and methane (CH_4), are also emitted in varying amounts [25]. Another near-term impact is glass-like ash emission. These ashes can be transported long-distance across continents and cause lethal pulmonary damage [26–29]. Ash plumes injected into the stratosphere and upper troposphere will scatter solar radiation (cooling), absorb heat, and perturb atmospheric circulation [30]. The shorter lifetime of volcanic ash due to gravitational deposition (compared to sulfate aerosols formed in the stratosphere) will generate more abrupt, short-lived cooling and complicated social and ecological consequences.

Is there any means to artificially counteract global cooling due to volcanic eruptions? Contemporary global warming has inspired investigations into intentional climate intervention (geoengineering), such as Solar Radiation Management, which aims to lower global temperatures through space mirror deployment (e.g., [31,32]), marine cloud brightening, or stratospheric aerosol injection (SAI) [33,34], which directly mimics volcanic cooling.

The conceptualization of counteracting global cooling has been presented in the literature, mostly qualitatively—such as releasing GHGs or heating aerosols as countermeasures in response to unilateral solar-radiation geoengineering [35], or injecting substances that bind to sulfate aerosols to reduce their atmospheric lifetime in response to large volcanic eruptions [11]. Others have even considered volcanic eruption prevention via engineering approaches of direct cooling subterranean magma chambers [22,36]. On the very long-term time scale, the idea of offsetting glacier cooling is also brought up [37].

The specific research question we consider here in this study is the following: could deliberate releases of GHGs reduce the magnitude of large volcanic cooling while minimizing undesirable side effects? To address this question, the global cooling due to a hypothetical large volcanic 2 Gt SO_2 injection is simulated using a simple climate model. This amount is comparable to the Yellowstone [9] or Toba eruptions [3], both estimated to have an SO_2 injection rate of 100× Pinatubo (with large uncertainty) and a Volcanic Explosivity Index (VEI) of 8. Our research extends Fuglestvedt et al. (2014) [38], which used a global climate model to simulate the role of chlorofluorocarbons in offsetting Tambora's cooling (VEI 7; [39]) by instead directly modeling an extensive suite of commercially available F-gases and identifying potential offsetting candidates. Additionally, a brief discussion is offered on the geophysical, technical, and economic constraints on production and the potential side effects of atmospheric chemistry. We are not recommending imminent, real-world preparations for deployment to be taken. Instead, we intend to motivate further study and

discussion of proactive mitigation of any global catastrophic risks—regardless of whether they are due to anthropogenic or natural causes.

2. Modeling Approach

2.1. Energy Balance Climate Model

We utilize a zero-dimension energy balance model called the Reduced compleXity Model (RXM), which is inspired by earlier works in the 1970s [40,41] and was developed by Ramanathan and Xu (2010) [42] and used in later studies (e.g., [2,43]). In a nutshell, with the evolution of mass emission over a certain time interval as the desired model input, atmospheric concentration, top-of-atmosphere (TOA) forcing (Wm^{-2}), and surface temperature response (°C) are estimated.

For methane, CH_4, mass emission is used to derive concentration ($C(t)$; unit: parts per billion [ppb]) with the following equation (Equation (1)).

$$C(t) = 715 + \left(\sum_{i=0}^{t} \frac{E[i]}{2.78} \times e^{\frac{-(t-i-1)}{\tau}}\right) - \left(715 \times \left(1 - e^{\frac{-t}{\tau}}\right)\right) \quad (1)$$

In Equation (1), E and t are the mass emission and time (in years) for a given year i, and τ is the perturbation lifetime of CH_4 (approximately 12 years per the Intergovernmental Panel on Climate Change [IPCC] Assessment Report 5 [AR5] and treated as a constant in this analysis without considering methane lifetime feedback at a different concentration) [44]. The conversion factor from the emission of 1 Mt to the atmospheric concentration of 1 ppb is 2.78 (ppb/Mt). We assumed a preindustrial concentration (avoiding the complexity of contemporary climate change) of 715 ppb and natural emissions of 100 Mt per year [44].

The direct forcing of CH_4 has a square root relationship with concentration ($F_D(t)$ in Equation (2), resulting in a marginally smaller response to concentration. We do not account for the overlapping effect with N_2O since N_2O is not modeled here. The indirect forcings due to atmospheric chemistry, such as stratospheric water vapor (0.07 Wm^{-2}), formation of CO_2 (0.016 Wm^{-2}), and tropospheric ozone (0.2 Wm^{-2}), are smaller in magnitude. Thus, they are scaled here from the CH_4 concentration linearly (Equations (3)–(5), for stratospheric water vapor, CO_2, and tropospheric ozone, respectively). The coefficients are obtained from IPCC AR5 WGI, Chapter 8, as their separate contributions to present-day (2005) forcing relative to the preindustrial (1850). The total forcing for CH_4 (F; unit: Wm^{-2}), on an annual basis (t), is then calculated in Equation (6).

$$F_D(t) = 0.57 \times \left(\frac{\sqrt{C(t)} - \sqrt{C_{1850}}}{\sqrt{C_{2005}} - \sqrt{C_{1850}}}\right) \quad (2)$$

$$F_{I1}(t) = 0.07 \times \left(\frac{C(t) - C_{1850}}{C_{2005} - C_{1850}}\right) \quad (3)$$

$$F_{I2}(t) = 0.016 \times \left(\frac{C(t) - C_{1850}}{C_{2005} - C_{1850}}\right) \quad (4)$$

$$F_{I3}(t) = 0.2 \times \left(\frac{C(t) - C_{1850}}{C_{2005} - C_{1850}}\right) \quad (5)$$

$$F(t) = F_D + F_{I1} + F_{I2} + F_{I3} \quad (6)$$

Fluorinated gases (F-gases) have been recognized as important contributors to global warming since the latter half of the 20th century, with radiative forcing currently equivalent to 18% of CO_2 despite concentrations at a million times smaller [45]. F-gases are widely used for refrigerants, fire suppression agents, and blowing foam insulation [46]. Most are non-toxic, non-flammable, and non-reactive. Other F-gases—especially HFCs—have increased in production after the agreement of the Montreal Protocol in 1987, which phased out the use of ozone-depleting Cl- and Br-bearing F-gases, including Chlorofluorocar-

bons (CFCs), hydrochlorofluorocarbons (HCFCs), and bromocarbons [47]. The increased use of hydrofluorocarbons (HFCs) is also a target of climate mitigation for the 21st century [46,48–50]. For the F-bearing compounds, concentration can be estimated from the time-varying emission and molar mass:

$$C(t) = C(t-1) + (E(t) \times \alpha) - C(t-1) \times (1 - e^{-\frac{1}{\tau}}) \quad (7)$$

In Equation (7), $E(t)$ is the emission amount at a given time step (in kt), and α is a mass conversion factor. The default time step is a day, considering their short lifetime of 0.5 to 3 years. Additional simulations using a longer time step of 1 month or 1 year were also tested for the shorter-lived Compound B (see below). This produced a high bias in concentration due to the omission of decay during the initial time step (the first month or the first year). Simulations using a time step of 1 day and 1 month largely converged (see further discussion later). The conversion factor between mass emission and atmospheric concentration, α, is the mixing ratio of 1 kt emission (10^9 g divided by m, molar mass in g/mol) with respect to the total molar count of the atmosphere. The final concentration is expressed in parts per billion (ppb), hence the multiplier of 10^9:

$$\alpha = \frac{\left(\frac{1 \times 10^9 \text{ g}}{m}\right)}{\left(\frac{5 \times 10^{21} \text{ g}}{28.97 \text{ g/mol}}\right)} \times \left(1 \times 10^9\right) \quad (8)$$

Conversion of concentration to radiative forcing is based on radiative efficiency ($\text{Wm}^{-2}\text{ppb}^{-1}$) [45]. Some saturation in absorption bands could occur, causing non-linearity. If so, the GHG radiative forcing contribution would increase at a lower rate. In that case, the necessary F-gas emissions estimated here will be biased low. However, the magnitude of this bias is difficult to quantify due to the need for more quantitative information in the literature.

In all cases (volcanic-related emissions, CH_4, and F-gases), we regard the forcing numbers as the instantaneous forcing at the TOA without considering the fast adjustment of clouds and stratosphere (effective radiative forcing). The total forcing generated by all compounds will collectively drive the temperature response using the following equation:

$$T(t) = T[0] + \sum_{0}^{i_t}\left(\frac{1 \text{ year}}{C_p \times \rho \times z} \times \left(F[i] - \frac{T[i]}{s}\right)\right) \quad (9)$$

where T and F are the temperature and forcing for a given year; C_p and ρ are the specific heat and density of seawater; z is the depth of the effective ocean mixed layer; s is climate sensitivity expressed in the unit of $^\circ\text{C}/(\text{Wm}^{-2})$. The time step in Equation (9) is one year. We do not directly implement the shorter (daily or monthly) time steps in the forcing-temperature response function of Equation (9) for three reasons. First, the radiative forcing formulation (concentration and forcing for CH_4 and F-gas) is based on empirical approximation at an annual mean (and global average) basis after accounting for the seasonal dependence of the background thermal radiation from the Earth that would affect the radiative efficiency. Second, the literature does not provide a large volcanic forcing time series in the necessary daily or monthly resolution. Third, the emission rate of F-gas is estimated to match the annual mean large volcanic forcing. Therefore, any bias in quantifying temperature response using the energy balance equation would operate equally in both the warming and cooling case and does not directly affect the emission estimates.

Regardless, as a robustness check, we implement a shorter time step (daily or monthly) in the emission–concentration relationship (Equation (7)) for one case. After calculating concentrations at the daily or monthly resolution, we convert it to an annual mean. We then perform a running average before quantifying its radiative forcing (using the formulations constructed on an annual mean basis) and temperature response (using Equation (9) at the annual time step).

2.2. Validation of the Climate Model

The 1991 eruption of Mt. Pinatubo injected ~20 Mt SO_2, the effects of which have been closely observed and extensively studied ([51–53]). Pinatubo observations test model fidelity (Figure 1), specifically the conversion of eruption-driven radiative flux anomalies into a global average temperature response.

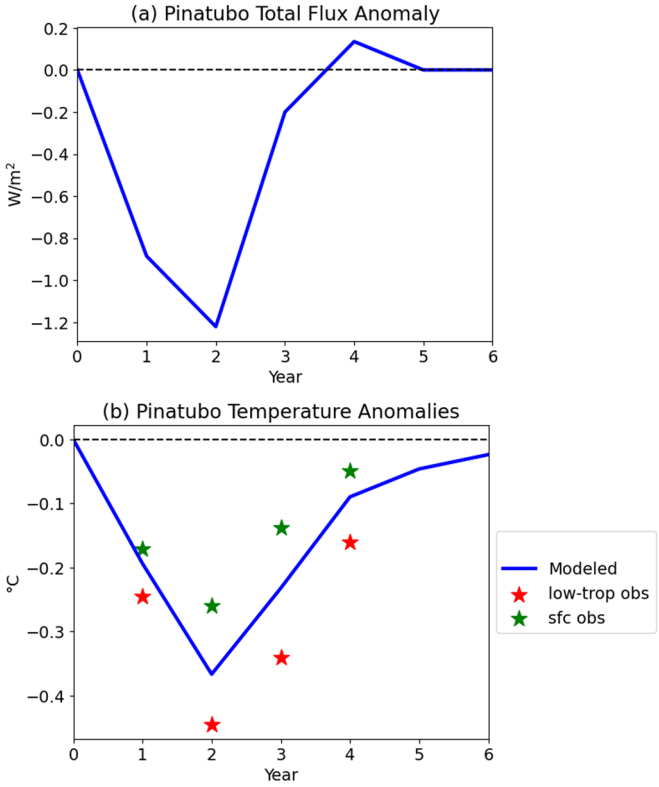

Figure 1. (**a**) Observed TOA (top of atmosphere) radiative flux anomaly following the Pinatubo eruption (shortwave and longwave, adopted from the monthly data as in Figure 1 of Soden et al., 2002 [53]). (**b**) Surface temperature response in our model, compared to the lower troposphere and surface observations [54]. Year Zero on the *x*-axis represents June 1990 to May 1991, the year preceding the eruption in June 1991.

Using observed monthly mean SW and longwave (LW) flux anomalies (60° S–60° N only), the annual average of total top-of-the-atmosphere (TOA) forcing is calculated and input (Figure 1a). The effective ocean mixed layer depth, denoted as z in Equation (9), is assumed to be relatively small (35 m), reflecting the short temporal scale of the Pinatubo eruption and, therefore, the limited role of oceanic thermal inertia. A climate sensitivity of 0.45 °C/Wm^{-2} (smaller than the 0.7–0.8 typically adopted for CO_2-induced climate change studies) is used because some positive climate feedback (e.g., ice-related surface albedo feedback) is not fully involved at a short timescale of 1–5 years. After running the model with these conditions, the simulated cooling largely agrees with the observed global average temperature drop of approximately 0.4 °C in Year 2, with a recovery curve also aligning closely with published data (Figure 1b) [53,54].

The model was also used to simulate the temperature response to a 2 Gt SO_2 emission scenario with a prescribed forcing (Figure 2a; [3]). While the prescribed forcing in Robock et al. (2009) [3] might be an overestimate according to other studies [24,55–57], this model tracks Robock et al.'s [3] published temperature response well, which was derived using a more complex global climate model. Here, we used a configuration of z = 50 m for the five years post eruption (Figure 2b). The effective ocean mixed layer depth (z) of 50 m is a reasonable assumption given the short duration of the forcing and agrees with Fuglestvedt et al. (2014) [38], who adopted a slab ocean model with a fixed depth of 54 m.

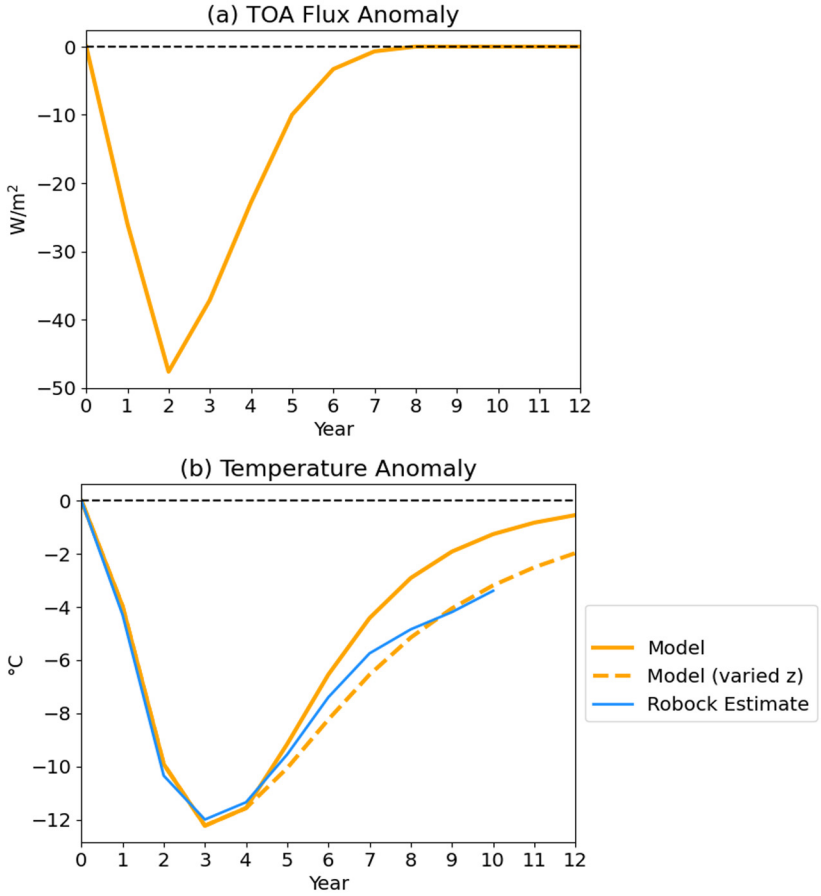

Figure 2. (**a**) TOA radiative forcing following a 2 Gt SO_2 injection (converted from the shortwave surface forcing estimates in Figure 4 of [3]). (**b**) Simulated global surface cooling (orange solid line) using the forcing estimates in (**a**), which is compared with Robock et al. (2009) [3] (blue solid line). The orange dash line is also simulated via our model, but assuming the effective ocean depth (z) increases from 50 to 80 m in Year 5.

The lack of a second (deeper) ocean box neglects the increasing role of the ocean in buffering the forcing and thus leads to a recovery (i.e., rebound from the cooling) that is faster than the recovery simulated in Robock et al.'s [3] coupled climate model. Recent works by the first author of this study used a two-box energy balance model with a coupled carbon cycle [58,59]. Since CO_2 emission is not directly relevant to this study, a simpler 1-box model was selected over the 2-box configuration. This 1-box model has also been used and validated extensively [2,48]. Careful comparisons between the two-box version and the more complex MAGICC model have been made [60]. Therefore, the utility and limitations of the 1-box model are well documented, and its application is justified here.

To fully demonstrate model sensitivity to the role of ocean heat content in buffering the response to forcing, Figure 2b shows temperature response assuming a larger effective ocean layer depth (80 m) after Year 5, which produces a better fit to the coupled ocean-atmosphere global climate model results. Similar to the timestep concern addressed above, the uncertainty of the assumption of effective ocean mixed layer depth (z) does not directly affect the derivation of required F-gas emission. This is because both the F-gas warming and volcanic cooling will change by the same fraction when a larger z is adopted. Ultimately, we only need to produce and maintain a close match between F-gas radiative forcing (heating) and volcanic forcing (cooling).

3. Results

3.1. Simulated Cooling in Response to a Large Volcanic Eruption

A large volcanic cooling event (e.g., a VEI of 8) has yet to be observed in recent history, so analyses must rely on mass flux approximations. Here, we adopt the lower estimate of 2 Gt SO_2 for the Toba eruption 74,000 before the present (100 × Pinatubo; [3]), which is also close to assumptions for the Yellowstone eruption [9]. There is no geological certainty of the magnitude of a large volcanic eruption. Some studies suggest Toba and other very large eruptions may be no more than 20 × the magnitude of Pinatubo [61], posing a smaller cooling crisis than analyzed here. For this prototype study, we only consider a hypothetical scenario rather than an accurate quantification of a particular large volcanic eruption.

Since our energy balance model cannot resolve the troposphere and stratosphere, forcing estimates from previous 3D modeling are used [3]. A large 50 Wm^{-2} TOA forcing (Figure 2a) is converted from the surface SW forcing time series presented in Robock et al. (2009)'s Figure 4 [3]. The conversion is needed to offset the LW warming effect of volcanic aerosols and stratospheric solar absorption. The conversion factor of 0.5 (Net_TOA/SW_Surface) is estimated by Timmreck et al. (2005) [9] and Timmreck et al. (2012) [15], suggesting a ratio of 0.4–0.6. Volcanic particulate matter (such as ash), CO_2, and H_2O emissions have been neglected here for simplicity. CO_2 emissions, even from large volcanic eruptions, have negligible impacts on the shorter timescale of years to decades [15,52] due to the much longer lifetime of CO_2 [62]. The H_2O intrusion into the stratosphere will produce some offsetting warming effect [63,64], but it is nearly insignificant compared to aerosol cooling unless under extreme conditions of tropopause collapse [65]. Volcanic ash plumes would exacerbate the abrupt cooling and also produce immediate damage; however, due to the limited quantification information found in the paleoclimate studies and the already large uncertainty of SO_2 injection amount, we defer the implementation of ash aerosols into a future study focusing on different types of volcanic eruptions (magnitude, composition, sequence, and duration).

Updated modeling with detailed microphysical aerosol processes [55] suggests a third of the cooling calculated within Robock et al. (2009) [3] due to its omission of sulfate aerosol size distribution dependence [15]. Nevertheless, our main purpose is to determine whether the concept of F-gas injection is generally feasible rather than targeting a particular global cooling scenario. Forthcoming studies should include more realistic scenarios with geological evidence, accounting for the large uncertainty of chemical compositions, forcing magnitude, and temporal sequences.

Figure 2b shows a global annual average temperature cooling of more than 10 °C following a 2 Gt SO_2 injection into the upper atmosphere. The temperature begins to recover from the initial cooling after three years, and the temperature gradually comes within 1 °C of the initial climate state approximately a decade after the eruption—emulating 3D global climate model outputs (dashed line in Figure 2b). Temperatures rebound as coagulation and precipitation of stratospheric sulfate aerosol occur. Given its magnitude, the comparatively short cooling period can still be globally disastrous, e.g., due to net primary productivity decline and crop yield losses.

The discrepancy between this model and Robock et al.'s [3] global climate model estimates as the temperature recovers (Figure 2b, after Year 6) is possibly due to fixing our effective ocean depth (z) to be constant throughout our simulation, rather than allowing it to increase (inherently accounted for in global climate models where a deeper ocean would have more heat inertia and therefore make the recovery from the imposed forcing slower). This model sensitivity is demonstrated in Figure 2b (see Methods). While not directly affecting the main results in the later section on the required mass of F-gases, this model limitation will need to be improved in future analyses, especially when considering the forcing sequence (e.g., multiple subsequent eruptions).

To comprehend the forcing and cooling rate, we first consider the possibility of directly releasing natural gas. Its main constituent, CH_4, has a GWP100 of 28 (global warming potential over the 100-year time scale being 28-times larger than CO_2) and a GWP20 of

84 [44]. Figure 3a shows this scenario; the required mass release of CH_4 is very large (200 Gt vs. current natural gas production of ~2.9 Gt/year (3.8 trillion cubic meters; [49])). Figure 3a shows that injected CH_4 cannot avoid "overshoot", as the initial success in offsetting the large volcanic cooling (despite an unrealistically high emission requirement) is followed by an overheating of more than 5 °C for many years, which would also be disastrous. The decadal lifetime of CH_4 is too long to counter an abrupt—yet temporary—cooling. Moreover, the actual CH_4 lifetime under such a large release would be even longer due to an associated reduction in atmospheric OH levels in response to the CH_4 injection (a primary CH_4 sink).

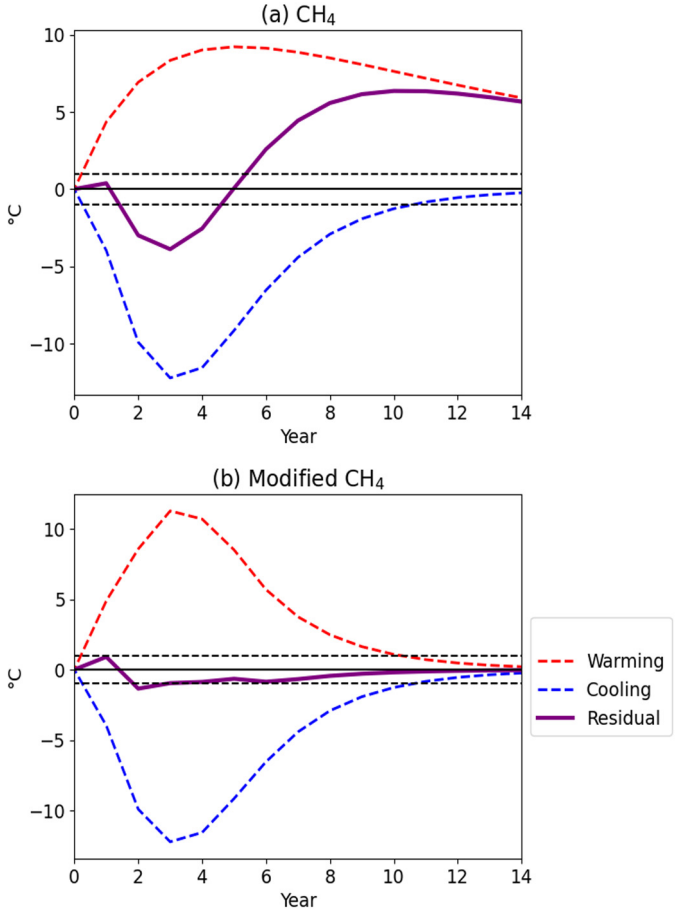

Figure 3. (**a**) Large volcanic cooling mitigation via a hypothetical 200 Gt CH_4 emission in Year 1, which is infeasible. The blue dashed line is cooling due to the volcanic eruption. The red dashed line is heating due to GHG release. The solid purple line represents the residual (i.e., summation of cooling and heating). Targeted [−1 °C, 1 °C] limits are shown as horizontal dashed black lines. The black solid line is the zero-line. (**b**) Similar mitigation via a 6 Gt "CH_4"-like emission (with stronger radiative efficiency and shorter lifetime) in Year 1, followed by 3.5 Gt releases in Years 2 and 3.

Matching the required response time of the volcanic cooling and the lifetime of warming agents is central to the selection of candidate gases. As a model sensitivity exercise, the CH_4 lifetime was lowered to 2 years. Radiative efficiency was simultaneously increased 35 times to 0.027 $Wm^{-2}ppb^{-1}$, testing whether the required mass release can be lowered correspondingly. The simulated temperature response obtained is encouraging. The temperature response curve of this "unstable and short-lived" designer compound (Figure 3b) is opposite to the large volcanic cooling with comparable magnitude and achieved at a much lower emission rate of 6 to 3.5 Gt in Years 1 and 2. This exercise prompted an examination of other existing short-lived compounds with higher radiative efficiency.

3.2. Temperature Responses to F-Gas Injections

HFCs have a wide range of atmospheric lifetimes (from months to 40 years) and global warming potentials (GWP100 ranging from <1 to 4790) [45]. Analysis of CH_4 (Section 2) suggests shorter lifetimes and higher radiative efficiencies are needed. Thus, in our selections, we deliberately exclude compounds with lifetimes longer than 3.5 years to mitigate the issue of persistent overheating. Excluding compounds with lifetimes below 0.5 years (reactive halogens, typically ranging from days to weeks) avoids the requirement for near-continuous releases. Ozone-depleting Br- and Cl-bearing gases and those containing oxygen atoms (due to their more complex structures) were also excluded from the current exploratory analysis. Table 1 lists the potential candidates from Hodnebrog et al. (2020) [45].

Table 1. A list of F-gas candidates ranked by lifetimes (0.5 to 3.2 years). The parameters are based on Hodnebrog et al. (2020) [45]. The five rows in boldface are compounds selected for further modeling analysis due to their higher GWP/lifetime ratio (A–E, ranked by this ratio from large to small).

Chemical Identifier	Formula (and Sum Form)	Molar Weight (g/mol)	Lifetime (Year)	Radiative Efficiency ($Wm^{-2}ppb^{-1}$)	GWP100	GWP100/ Lifetime
HFC-152	CH_2FCH_2F ($C_2H_4F_2$)	66	0.5	0.05	23	46
1,3,3,4,4,5,5-heptafluoro cyclopentane	$CF_2CF_2CF_2CF{=}CH$ (C_5HF_7)	194	0.6	0.21	47	78
1,3,3,4,4-pentafluorocyclobutene (A)	**$CH{=}CFCF_2CF_2$ (C_4HF_5)**	144	**0.7**	**0.27**	**97**	**139**
Hexafluorocyclobutene(B)	**$CF{=}CFCF_2CF_2$ (C_4F_6)**	162	**1**	**0.3**	**132**	**132**
HFC-263fb	$CH_3CH_2CF_3$ ($C_3H_5F_3$)	98	1.1	0.1	78	71
Octafluorocyclopentene	$CF_2CF_2CFCF_2CF_2$ (C_5F_9)	231	1.1	0.25	82	75
1,1,2,2,3,3-hexafluorocyclopentane	$CF_2CF_2CF_2CH_2CH_2$ ($C_5H_4F_6$)	178	1.6	0.2	126	79
HFC-152a (C)	**CH_3CHF_2 ($C_2H_4F_2$)**	66	**1.6**	**0.1**	**172**	**108**
HFC-41 (E)	**CH_3F (CH_3F)**	34	**2.8**	**0.02**	**142**	**51**
1,1,2,2,3,3,4-heptafluorocyclopentane	$CF_2CF_2CF_2CHFCH_2$ ($C_5H_3F_7$)	196	2.8	0.24	243	87
HFC-245ea	$CHF_2CHFCHF_2$ ($C_3H_3F_5$)	134	3.2	0.16	267	83
HFC-245eb (D)	**$CH_2FCHFCF_3$ ($C_3H_3F_5$)**	134	**3.2**	**0.2**	**341**	**107**
1,1,2,2,3,3,4,5-octafluorocyclopentane	$CF_2CF_2CF_2CHFCHF$ ($C_5H_2F_8$)	214	3.2	0.26	271	85

The candidates in Table 1 were further narrowed by selecting those with a higher GWP100/lifetime ratio (rightmost column). GWP100/lifetime was used as the ranking criterion over GWP100 for multiple reasons. First, GWP100 represents integrated forcing (akin to temperature response) over 100 years. Second, GWP100/lifetime is sensitive to both radiative efficiency and lifetime, as opposed to only radiative efficiency. Third, GWP100 alone does not closely correlate with near-term warming (a few years after emission), which is the focus of this study. Assuming the same radiative efficiency and molar weight, the same instantaneous mass release will last longer in the atmosphere with a longer lifetime and will produce larger warming over 100 years (hence a larger GWP100).

The release of the top five compounds was modeled separately. The model was run numerous times for each compound, with the magnitude and timing of emissions adjusted after each run to approach a minimized temperature residual—defined as within a ± 1 °C of the pre-eruption level throughout the entire post-eruption recovery (Figure 4a–e). We dis-

cuss the properties of these five identified compounds below, ordered by GWP100/lifetime ratio (Table 1).

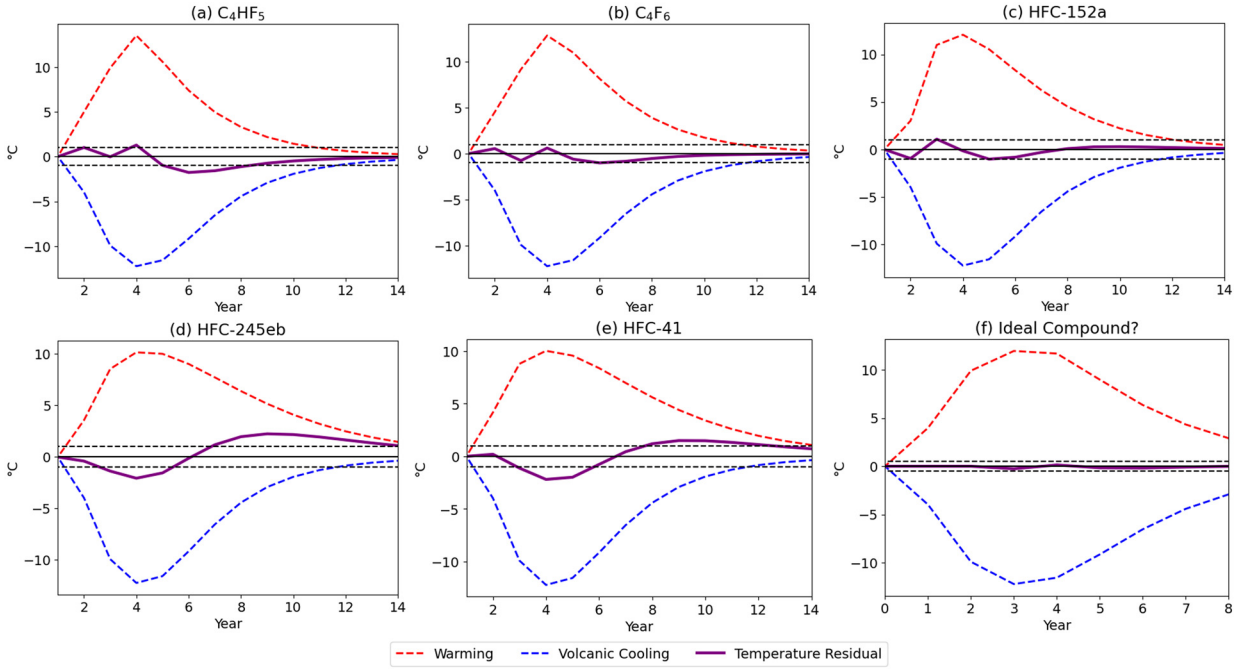

Figure 4. Simulated volcanic cooling and warming offset by F-gas emission. (**a**) C_4HF_5; (**b**) C_4F_6; (**c**) HFC-152a; (**d**) HFC-245eb; (**e**) HFC-41 (CH_3F); and (**f**) a possible compound with ideal characteristics. The blue dashed line is cooling due to volcanic eruption. The red dashed line is heating due to F-gases. Each purple solid line represents the residual (net temperature effect. Targeted [−1 °C, 1 °C] limits are shown as horizontal dashed black lines. The black solid line is the zero-line. Note that in (**f**), the timeline is shortened to Years 0 to 8 to demonstrate a clear optimal counterbalancing by the 'ideal' compound.

Compound A, C_4HF_5 (Pentafluoro-cyclobutene in Figure 4a), has a lifetime of 0.7 years and a GWP100 of 97. Emission deployment after optimization is 6.0 Gt in Year 1 and 6.5 Gt in Years 2–3 (Figure 5a), distributed evenly over 365 days of a year. The response residual after mitigation ranges from −1.4 to 0.9 °C (Figure 5b). Its lowest GWP and shortest lifetime (among the five compounds tested here) necessitate greater total emissions to offset the specific cooling.

Compound B, C_4F_6 (Hexafluoro-cyclobutene; Figure 4b), has a lifetime of 1 year and a GWP100 of 132. In order to offset the cooling, it requires an emission deployment of 8.25 Gt in the Year 1 post-eruption, followed by 2.75 Gt in Years 2–3 (Figure 5a). This is a promising candidate, offsetting the cooling almost entirely, with the residual falling within a 1 °C level (Figure 5b).

Compound C, CH_3CHF_2 (HFC-152a in Figure 4c), has a lifetime of 1.6 years and GWP100 of 172. The optimized emission sequence is 5.6 Gt in Year 1 and 5.5 Gt in Year 2. Similar to C_4F_6, HFC-152a can greatly offset cooling with a slightly less massive emission, maintaining a residual within ±1 °C.

Compound D, $CH_2FCHFCF_3$ (HFC-245eb in Figure 4d), has a lifetime of 3.2 years and a GWP100 of 341. It only needs a single-year release of 6.75 Gt in Year 1 alone—greatly reducing the reliance on social and industrial infrastructure survivability. The longer lifetime and larger GWP enable the least amount of total mass release. However, the temperature response residual is less ideal (in contrast to A with the shortest lifetime) and can be as large as 1.3 to 2.6 °C.

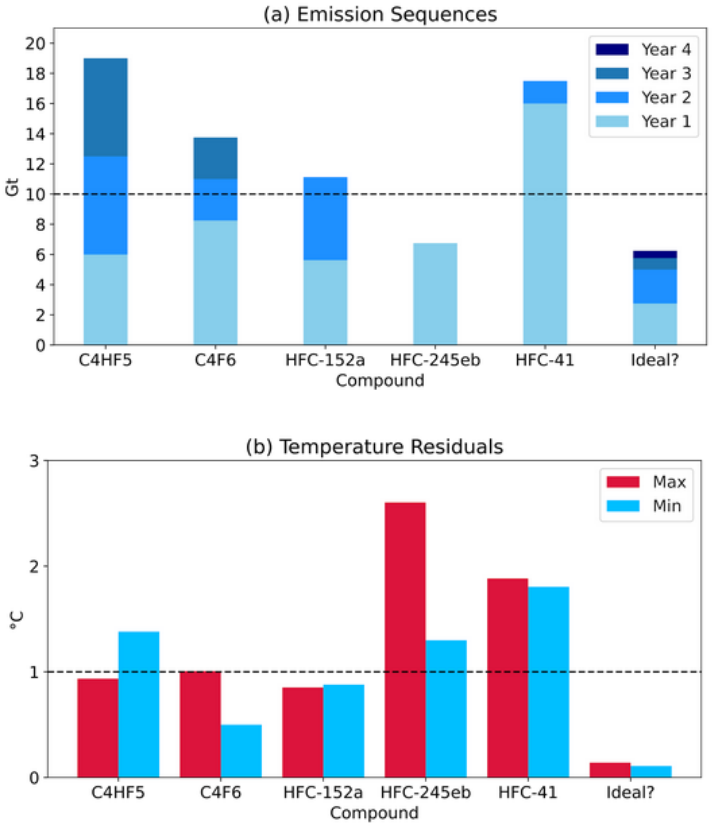

Figure 5. (**a**) The sequencing of annual emission of the five identified compounds and the "ideal" compound. The emission sequence is constructed via simple model runs with optimized results shown in Figure 4. (**b**) The range of temperature residuals as seen in Figure 4, which is targeted to be kept below 1 °C.

Compound E, CH_3F (HFC-41 in Figure 4e), has a lifetime of 2.8 years and GWP100 of 142. This compound requires the largest release rate (16 Gt in Year 1; 1.5 Gt in Year 2) due to its low radiative efficiency (an order of magnitude smaller than Compound D of HFC-245eb, Table 1). This deficiency is offset by a longer lifetime, hence the relatively large GWP. Although the temperature residual is one of the least ideal among other compounds, its chemical simplicity may imply smaller production costs and environmental effects (see Sections 4 and 5).

Compounds with lifetimes below two years (A, B, and C) and higher GWP/lifetime ratios offer more satisfactory emission sequences and temperature residuals (Figures 4 and 5). Moreover, C_4F_6 and HFC-152a reduce the eruption-induced cooling to within a 1 °C range for the entire experiment period. In contrast, D and E's lower GWP/lifetime ratios produce undesirable cooling and warming due to an excessive lifetime. This is especially apparent for HFC-245eb in Figure 4d, despite it having the highest GWP of the tested compounds.

Additionally, the metric of integrated radiative forcing can be used to interpret the temperature response to diverse compounds (Figure 6). Radiative forcing (Figure 6b) and integrated radiative forcing (Figure 6c) are shown for two representative F-gases with similar GWP (to contrast with the volcanic forcing also plotted in Figure 6b,c). Total mass releases of HFC-41 and C_4F_6 are 14 Gt and 8.3 Gt, respectively, despite similar GWPs (142; 132). The resulting volume concentrations differ by roughly an order of magnitude (Figure 6a) due to HFC-41's much smaller molar weight. However, both instantaneous and integrated radiative forcings are similar, given C_4F_6's larger radiative efficiency (Table 1).

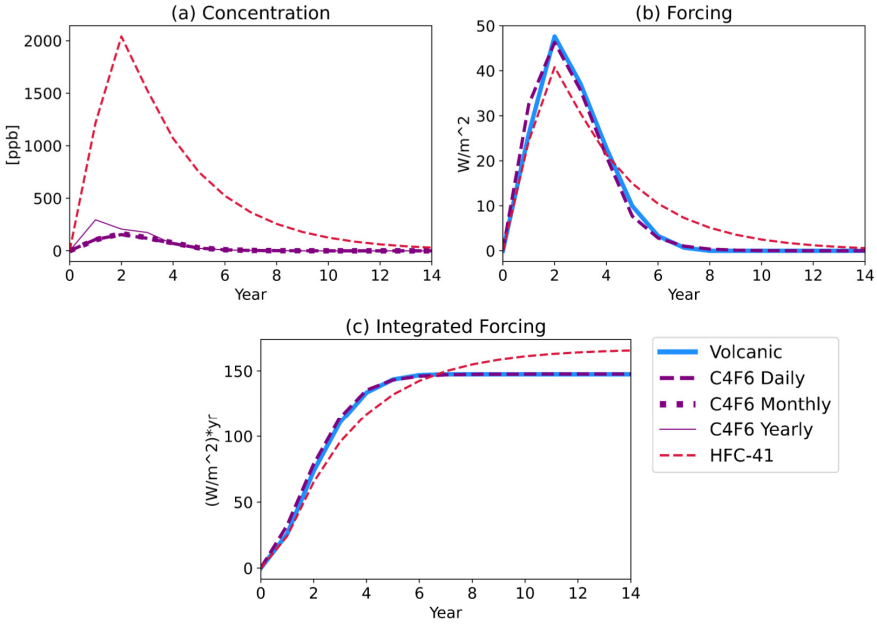

Figure 6. (**a**) Simulated average atmospheric concentrations of C_4F_6 (Compound B, purple dashed line) and HFC-41 (Compound E, red dashed line). For the shorter-lived C_4F_6, results using monthly (purple dot–dash line) and yearly (purple solid line) time steps, respectively, are shown as a robustness check. The monthly time steps show very good agreement with the default results using daily steps (purple dashed line), while the yearly time steps produce a concentration that is biased high. (**b**,**c**) simulated radiative forcing and integrated radiative forcing, respectively, of C_4F_6 (Compound B, purple dashed line C_4F_6 daily) and HFC-41 (Compound E, red dashed line). Volcanic forcing (blue solid lines), as in Figure 2, is plotted with the sign reversed for easy reference and comparison.

The integrated radiative forcing in Figure 6c can approximate the temperature counterbalance well for short-lived gases. The difference in temporal response is also consistent with the temperature simulation in Figure 4. For example, HFC-41 (red) shows an initial underheating followed by an overheating (Figure 6c). C_4F_6 maintains a closer mirroring of integrated forcing with respect to volcanic eruptions (Figure 6c, blue)—also shown in the match of temperature trajectories up to Year 4, after which an under-compensation is found.

While these five shortlisted compounds show promise in mitigating most of the cooling, they are designed and manufactured for different purposes and are clearly not ideal. We lastly discuss the possibility of a designer compound (Figure 4f) that can be tuned to produce the desired cooling mitigation (residual < 0.5 °C)—statistically indistinguishable from interannual climate variability. As an exploratory exercise, this "ideal" compound is speculated to possess the largest radiative efficiency of 0.3 $Wm^{-2}ppb^{-1}$ found in C_4F_6 (Figure 4b) while maintaining a small molecular weight of 67, similar to HFC-152a (Figure 4c). Fine-tuning the mass emission sequences to achieve the right amount of warming (Year 1–4 at 2.75 Gt, 2.25 Gt, 0.75 Gt, and 0.5 Gt, respectively; the rightmost bar in Figure 5a) suggests a lifetime of ~0.9 years—between that of C_4HF_5 (Figure 4a) and C_4F_6 (Figure 4b).

Overall, our detailed modeling provides an order-of-magnitude quantification of the effect of releasing greenhouse gases (CH_4 and particularly fluorinated gases) in balancing global cooling due to potentially large SO_2 injection during super volcanic emissions. The tested five species of fluorinated gases can largely offset the global cooling effect caused by volcanic eruptions, whereas the longer-lived compounds, such as CH_4, are not suitable to offset the cooling efficiently. While we refrain from making recommendations on the elemental composition and molar structure, the identified characteristics (molar weight, radiative efficiency, and lifetime) above are similar to those existing, suggesting the possibility of designing an "ideal" compound mixture.

4. Model Uncertainty, Limitation, and Potential Next Steps

4.1. Limitations Due to Geophysical, Technical, and Economic Constraints

Fluorine used to manufacture F-gases is extracted from mined fluorspar (CaF_2) and fluorapatite ($Ca_5(PO_4)_3F$) ores [66]. Post extraction, these minerals are directly refined (fluorspar) or chemically converted (fluorapatite) into pure CaF_2, the primary material in the production of F-bearing gases [66]. There is an estimated 5 Gt of CaF_2 equivalent extractable reserve on the Earth (USGS, 2020), which is about 2.5 Gt of F-equivalent. Based on our calculation, HFC-245eb requires the least amount of elemental fluorine (70% of its total mass), about 4.2 Gt in total (all needed in Year 1). Yet, this elemental fluorine mass is at least three orders of magnitude larger than the present-day production of about ~7 Mt annually [67].

The required production would consume nearly all currently estimated global CaF_2 reserves, but mineable reserves may increase with future exploration [68]. This constraint may be alleviated by tapping into the ocean-based source. Approaches to extracting dissolved F ions from the ocean exist [69], but a close examination of technical details and costs is beyond the scope of this paper. The fluorine content of seawater ranges between 1 and 1.4 mg/L [66]. Presuming a mineable shallow (300 m) surface ocean with a volume of roughly 100 million km^3, up to 150 Gt of fluorine could be extracted, far more than the required F mass of the single-digit Gt scale.

Jaccaud et al. (2020) [66] placed the price of elemental fluorine (F, molar weight = 19 g/mol) at USD 5–8 per kilogram, based on extracting from mineral sources only, not the ocean. As a rough estimate, adopting the value of USD 2.5 per kilogram (presuming future economies of scale) and also doubling this cost to account for the manufacturing of fluorinated compounds, the price for the compound with the smallest F requirement out of the five compounds tested (HFC-245eb), 4.8 Gt during the deployment phase, would cost a total of USD ~24 trillion in total. When spread out over the decade dealing with the crisis, the annualized cost is about 10% of the United States GDP and on par with current global military spending—a measure potentially justifiable and feasible as an alternative to global civilization collapse.

Considering the lead time for scaling production, studies have shown that extreme magnitude eruptions are likely preceded by some geologic signals [70], providing possible predictability. However, given the limited monitoring capacity and unknown factors contributing to eruptive timing and magnitude, the range of lead times is wide—from days to decades [70,71]. In an optimistic scenario with ample lead time, F-gas stockpiles could be manufactured in advance. Such an enormous accumulation of F-gas would be a project with great economic, engineering, and security complexities. A thorough cost–benefit analysis would require in-depth collaboration between climatologists and experts in these fields, which is beyond this proof-of-concept study.

This analysis identified properties of a single candidate; however, a cocktail of novel "designer" compounds (fluorinated or not)—with enhanced absorption efficiency, mixed lifetimes, and reasonable production cost—could be developed and manufactured. Similar proposals exist in the context of geoengineering [72] and counter-geoengineering [35]. Detailed analyses to assess such strategies' technological and economic feasibility are anticipated in the future.

4.2. Limitation Due to Chemical Complexities

Gigaton-scale releases of compounds containing C-H bonds could also disrupt the tropospheric chemistry of the hydroxyl radical (OH). A large depletion of tropospheric OH could exacerbate air pollution caused by primary emissions of CO and VOCs by increasing their lifetimes. The OH loss rate due to F-gases can be calculated and compared to the loss rate due to background CH_4 and CO abundance at ~1 s^{-1} ([73,74]). OH decay rate perturbation due to fluorinated gases (F-gases) is detailed below. The enhanced decay rate of OH (in s^{-1}) due to a specific F-gas is estimated using $(d[OH]/dt)/[OH] = -k(\text{F-gas}) \times [\text{F-gas}]$, where [OH] and [F-gas] is the molecular density (number of molecules per cm^3)

and k(F-gas) is the reaction rate constant in cm^3/molecules/s. k(F-gas) is estimated by 1/(lifetime×[OH]) without considering temperature dependence, where the average global [OH] is ~10^6 molecules/cm^3 [73]. [F-gas] is calculated from the mixing ratio multiplied by atmospheric molecular density (~2.5×10^{19} molecules/cm^3). The background OH decay rate, primarily due to atmospheric CO and CH_4, is similarly based on [CO] and [CH_4], as well as k(CO) and k(CH_4) [73].

Our model estimates approximately a 100 to 150 ppb initial abundance of C_4F_6 after release and instantaneous dilution (Figure 6a)—equivalent to a 0.1 to 0.15 s^{-1} OH reactivity. This is equivalent to a 10–15% drop from background levels, which can significantly increase CH_4 lifetime. Reductions in OH due to F-gas oxidation, followed by an increase in the lifetime of background CH_4, would induce additional warming and imply less F-gas would be needed. In the case of CH_3F (HFC-41), our calculation (Figure 6a) shows the average tropospheric mixing ratio would be as high as 2000 ppb, creating an OH loss rate of ~0.6 s^{-1}, more disruptive than C_4F_6. However, even assuming the 60% drop in OH and subsequent CH_4 lifetime increase, this would only lead to roughly a doubling of CH_4 concentration from the background level, elevated during the source of operations. Following Equation (6), this higher CH_4 concentration would only translate to a radiative forcing of 0.5 Wm^{-2}, almost two orders of magnitude smaller than the direct forcing due to F-gases (Figure 6b).

The initial shock of the volcanic eruption could already greatly perturb the atmospheric chemistry, in addition to producing undesired cooling. The F-gases' lifetime in the atmosphere is predominantly determined by their reactions with OH, which can change due to solar radiation changes induced by volcanic aerosols. Moreover, stratospheric ozone loss will likely increase the OH production in the troposphere due to increased photolysis rates. These will also indirectly impact the lifetime of F-gases (additional to the lifetime feedback due to F-gas itself), hence the required emissions profile.

We can also speculate that chemical interactions between F-gas releases and volcanic SO_2 emissions could lead to secondary side effects on atmospheric chemistry. F-gases may alter SO_2 and sulfate lifetimes, with consequences for cooling and recovery timelines. The oxidation of released F-gas could lead to slower SO_2 oxidation (due to lower OH levels) to form sulfate aerosols and thus mute the volcanic cooling response, similar to the competing effects of a large volcanic eruption itself leading to slower SO_2 oxidation [75]. Dynamically, the tropospheric warming due to F-gases may alter circulation patterns, changing the lifetime of stratospheric aerosols.

These complex chemical and dynamic interactions (including what the eruption does to stratospheric ozone and, hence, tropospheric photolysis rates affecting the OH and F-gas lifetimes) cannot be fully accounted for and incorporated into this simple 'toy' climate modeling analysis with back-of-the-envelope chemistry calculations.

Other adverse environmental and health impacts could result from first- or second-order F-gas reaction products, which may be toxic. FHCO, the first reaction product of CH_3F, may accumulate near release sites; its aqueous formation of HF could have health and environmental effects due to gas-phase exposure or acid rain. These ecological risks need to be mitigated by monitoring and facilitating the mineralization of fluorine upon degradation from the injected gases. However, the adverse perturbations to biogeochemical cycling need to be placed in the context of the disruption caused by large volcanic eruption, which would have already significantly disrupted the stratospheric ozone layer and tropospheric chemistry, followed by acid rain and tropospheric haze due to aerosol fallout.

4.3. Limitation Due to the Spatial Distribution of Temperature Response

Despite successfully rebalancing global mean temperature using F-gas releases, a mismatch in spatial distribution would be unavoidable. Previous studies found relative underheating in the tropics, where aerosol-induced surface cooling is stronger than at higher latitudes [38]. Vertically, some overheating is possible in the stratosphere—where volcanic aerosols lead to strong, local heating—as well as a warming of the tropopause and disruption of typical stratospheric dynamics, especially if volcanic dust is included in the

model. These spatial mismatches are known issues for SAI, and potential fixes have been proposed via a strategic release in a specific latitude, altitude, and season [76–79]. A similar strategy with multi-location (varying latitudes) surface release could be employed with F-gases, given their similarly short lifetimes. More complex modeling strategies must be used to test these possibilities, such as energy balance models with higher dimensions [80] or a global climate model [38].

Fuglestvedt et al. (2014) [38] used a global climate model with a spatial resolution of $1.9^\circ \times 2.5^\circ$, providing valuable insights into regional and hydrological impacts; however, it was unsuited for screening candidate compounds due to computational resource constraints. This analysis also advances beyond Fuglestvedt et al. (2014) [38], because the previous study only considered a much smaller eruption (3 times of the magnitude of the 1991 Pinatubo eruption), a single hypothetical compound (with radiative properties equivalent to CFC-11, but a shorter lifetime and no impact on stratospheric ozone), and only briefly discussed side effects.

4.4. Limitation Due to Model Simplicity and Future Plans

Nevertheless, we acknowledge that the simple model analysis is inadequate to capture the complexity of some involved atmospheric processes, such as the full feedback due to chemistry and dynamics, and a future project using an Earth system model with the carbon cycle and interactive tropospheric chemistry (OH and CH_4 responses to other perturbations), and especially with a good presentation of stratospheric chemistry and dynamics, would be ideal for verifying the "order of magnitude" estimates provided here that are largely speculative.

Due to the complexity involved, simple climate modeling should be carried out again using a full chemistry–climate model to capture the evolution of these short-lived gases and aerosols under the perturbed climate following a volcanic eruption. There are two potential directions moving forward:

(a) A proper Earth system model with fully coupled biosphere and chemistry can be adopted, even at a low spatial resolution. However, no existing Earth system models have incorporated the interactive chemistry for these short-lived F-gases. They typically prescribe 2–3 long-lived CFCs in atmospheric concentrations, which would prevent the tests of compounds with various lifetimes as this study provided. Potentially, with the preliminary result and ballpark estimates here, the community will have a stronger interest in adding F-gases as active tracers to understand their GHG effects better. These active F-gases can then be added to some existing volcanic eruption simulations (e.g., Pinatubo or larger ones) to quantify the cooling offset, with a more realistic consideration of zonal circulation as well as land–ocean temperature contrasts;

(b) A 1D column radiative–convective equilibrium model can also be used to address the issues related to lapse rate changes under a very large volcanic eruption. However, to the best knowledge of the authors, those radiative transfer models are not readily equipped with the stratospheric chemistry needed to account for processes such as stratospheric aerosol plumes and layers or photolysis rates affecting trace gases' lifetime and their vertical distribution. Moreover, they are not typically coupled with an ocean model at the bottom, so they cannot simulate the temporal evolution of warming/cooling, which is the central theme of our paper. Future model development efforts are needed to build a modeling tool that can be used for testing the ideas in this paper.

We note that performing the same set of calculations with Earth system models would be very time-consuming and computationally expensive, and the simple modeling exercise gives a first look at the possibility and lays the foundation for requesting resources to continue this line of investigation.

5. Conclusions

The biosphere and human society face a potential threat from future large and even "super" volcanic eruptions. These eruptions would inject substantial amounts of SO_2 and other substances into the atmosphere, potentially causing global cooling comparable to the Toba eruption. We propose that releasing specific chemical compounds into the atmosphere could mitigate this cooling effect and its consequences. Due to the uncertainties surrounding the magnitude of such eruptions, we conduct a proof-of-concept test by considering a hypothetical injection of 2 Gt of SO_2 to simulate the potential impact of a "supervolcanic" eruption (while disregarding complexities such as ash and water vapor emissions). This analysis identifies a group of F-gas compounds that could be released on a large scale and are capable of counterbalancing the cooling effects of the SO2 released during such a hypothetical eruption—thereby potentially significantly mitigating its impact.

We examined a suite of commercially available F-gases with varying radiative efficiency and lifetime. We then identified a few leading candidates (Table 1). Specifically, we examined the suite of F-gases in Hodnebrog et al. (2020) [45] with lifetimes between 0.5 and 3.5 years to avoid the issues of persistent overheating and continuous deployment. Br- and Cl-bearing gases were excluded (due to ozone depletion), as well as those containing oxygen (due to their more complex structure). Selected gases would need to be manufactured, potentially stocked, and released at a Gt scale to counterbalance a Yellowstone-like, large volcanic eruption. We found that even after such a large-scale eruption, the residual temperature changes could be kept within typical year-to-year natural variability. The desired physical and chemical properties of an "ideal compound" were identified. Such a compound would almost completely offset the known cooling, when released in subsequent years after the eruption. The actual selection of compound(s) and the necessary mass release is dependent on the specific volcanic cooling. Longer-lived greenhouse gases such as methane are unsuitable for this purpose due to the short-term nature of volcanic cooling.

While "ideal" compounds (or their combinations) with Gt-scale release appear capable of offsetting the volcanic cooling, limitations and caveats include the production limitations (due to the geophysical constraints on mineral availability) as well as the technical and economic constraints (estimated based on the current market). While future technological developments could relax some of these constraints, the environmental consequences of a massive F-gas release—on both the perturbation to the atmospheric oxidation capacity and precipitation acidification, as well as the spatial pattern of temperature responses—need further scrutiny. However, these side effects may be tolerable in comparison to the immense consequences of unmitigated cooling.

The analysis presented here suggests global catastrophic risks due to abrupt cooling could at least be partially mitigated with geoengineering. Due to the prototypical nature of this analysis, here we do not suggest real-world deployment. Producing massive amounts of F-gas seems to be limited by land-based mineral availability, and further economic analysis is hindered by the technical uncertainty in oceanic extraction. Moreover, due to the large uncertainty of cooling magnitude, preemptive manufacturing and large-scale stockpiling are needed. Still, no assessment is available on technical solutions for transport and storage, as well as associated risks such as inadvertent leakage.

Barring large uncertainties in the modeling and omitted factors (e.g., dust/ash emissions), this study advances the necessary discussion regarding proactive mitigation of global catastrophic risks and aims to inspire more research in this direction. To safeguard the long-term continuity of human civilization, such forward-thinking should not be restricted [81].

Author Contributions: Y.X. conceived the study. N.P.R. did the modeling analysis. Y.X., N.P.R., J.S., and A.J.L. wrote the paper with input from all other co-authors (G.W.S., Y.G.Z., P.Y., J.H., G.J.M.V.). All authors have read and agreed to the published version of this manuscript.

Funding: This research received no external funding.

Institutional Review Board Statement: Not applicable.

Informed Consent Statement: Not applicable.

Data Availability Statement: The datasets used and/or analyzed during the current study are available from the corresponding author on reasonable request.

Acknowledgments: We are grateful for the comments and encouragement from Gabrielle Dreyfus, Gerald North, Zachary McGraw, and Brian Toon.

Conflicts of Interest: The authors declare no conflicts of interest.

References

1. Ripple, W.J.; Wolf, C.; Lenton, T.M.; Gregg, J.W.; Natali, S.M.; Duffy, P.B.; Rockström, J.; Schellnhuber, H.J. Many risky feedback loops amplify the need for climate action. *One Earth* **2023**, *6*, 86–91. [CrossRef]
2. Xu, Y.; Ramanathan, V. Well below 2 °C: Mitigation strategies for avoiding dangerous to catastrophic climate changes. *Proc. Natl. Acad. Sci. USA* **2017**, *114*, 10315–10323. [CrossRef] [PubMed]
3. Robock, A.; Ammann, C.M.; Oman, L.; Shindell, D.; Levis, S.; Stenchikov, G. Did the Toba volcanic eruption of ∼74 ka B.P. produce widespread glaciation? *J. Geophys. Res.* **2009**, *114*, D10107. [CrossRef]
4. Coupe, J.; Bardeen, C.G.; Robock, A.; Toon, O.B. Nuclear Winter Responses to Nuclear War Between the United States and Russia in the Whole Atmosphere Community Climate Model Version 4 and the Goddard Institute for Space Studies Model E. *J. Geophys. Res. Atmos.* **2019**, *124*, 8522–8543. [CrossRef]
5. Bostrom, N.; Ćirković, M.M. *Global Catastrophic Risks*; Oxford University Press: Oxford, UK, 2008.
6. Mills, M.J.; Toon, O.B.; Lee-Taylor, J.; Robock, A. Multidecadal global cooling and unprecedented ozone loss following a regional nuclear conflict. *Earth's Futur.* **2014**, *2*, 161–176. [CrossRef]
7. Vellekoop, J.; Sluijs, A.; Smit, J.; Schouten, S.; Weijers, J.W.H.; Damsté, J.S.S.; Brinkhuis, H. Rapid short-term cooling following the Chicxulub impact at the Cretaceous–Paleogene boundary. *Proc. Natl. Acad. Sci. USA* **2014**, *111*, 7537–7541. [CrossRef]
8. Bardeen, C.G.; Garcia, R.R.; Toon, O.B.; Conley, A.J. On transient climate change at the Cretaceous−Paleogene boundary due to atmospheric soot injections. *Proc. Natl. Acad. Sci. USA* **2017**, *114*, E7415–E7424. [CrossRef]
9. Timmreck, C.; Graf, H.-F. The initial dispersal and radiative forcing of a Northern Hemisphere mid-latitude super volcano: A model study. *Atmos. Chem. Phys.* **2006**, *6*, 35–49. [CrossRef]
10. Black, B.A.; Lamarque, J.-F.; Marsh, D.R.; Schmidt, A.; Bardeen, C.G. Global climate disruption and regional climate shelters after the Toba supereruption. *Proc. Natl. Acad. Sci. USA* **2021**, *118*, e2013046118. [CrossRef]
11. Cassidy, M.; Mani, L. Huge volcanic eruptions: Time to prepare. *Nature* **2022**, *608*, 469–471. [CrossRef]
12. Stocker, M.; Steiner, A.K.; Ladstädter, F.; Foelsche, U.; Randel, W.J. Strong persistent cooling of the stratosphere after the Hunga eruption. *Commun. Earth Environ.* **2024**, *5*, 450. [CrossRef]
13. Inguaggiato, S.; Liotta, M.; Rouwet, D.; Tassi, F.; Vita, F.; Schiavo, B.; Ono, S.; Keller, N.S. Sulfur origin and flux variations in fumarolic fluids of Vulcano Island, Italy. *Front. Earth Sci.* **2023**, *11*, 1197796. [CrossRef]
14. Ding, S.; Plank, T.; Wallace, P.J.; Rasmussen, D.J. Sulfur_X: A model of sulfur degassing during magma ascent. *Geochem. Geophys. Geosyst.* **2023**, *24*, e2022GC010552. [CrossRef]
15. Timmreck, C.; Graf, H.-F.; Zanchettin, D.; Hagemann, S.; Kleinen, T.; Krüger, K. Climate response to the Toba super-eruption: Regional changes. *Quat. Int.* **2012**, *258*, 30–44. [CrossRef]
16. Self, S.; Rampino, M.R.; Newton, M.S.; Wolff, J.A. Volcanological study of the great Tambora eruption of 1815. *Geology* **1984**, *12*, 659. [CrossRef]
17. Scherrer, K.J.; Harrison, C.S.; Heneghan, R.F.; Galbraith, E.; Bardeen, C.G.; Coupe, J.; Jägermeyr, J.; Lovenduski, N.S.; Luna, A.; Robock, A.; et al. Marine wild-capture fisheries after nuclear war. *Proc. Natl. Acad. Sci. USA* **2020**, *117*, 29748–29758. [CrossRef]
18. Da, Y.; Xu, Y.; McCarl, B. Effects of Surface Ozone and Climate on Historical (1980–2015) Crop Yields in the United States: Implication for Mid-21st Century Projection. *Environ. Resour. Econ.* **2021**, *81*, 355–378. [CrossRef]
19. Jägermeyr, J.; Robock, A.; Elliott, J.; Müller, C.; Xia, L.; Khabarov, N.; Folberth, C.; Schmid, E.; Liu, W.; Zabel, F.; et al. A regional nuclear conflict would compromise global food security. *Proc. Natl. Acad. Sci. USA* **2020**, *117*, 7071–7081. [CrossRef]
20. Xia, L.; Robock, A.; Scherrer, K.; Harrison, C.S.; Bodirsky, B.L.; Weindl, I.; Jägermeyr, J.; Bardeen, C.G.; Toon, O.B.; Heneghan, R. Global food insecurity and famine from reduced crop, marine fishery and livestock production due to climate disruption from nuclear war soot injection. *Nat. Food* **2022**, *3*, 586–596. [CrossRef]
21. Kandlbauer, J.; Hopcroft, P.O.; Valdes, P.J.; Sparks, R.S.J. Climate and carbon cycle response to the 1815 Tambora volcanic eruption. *J. Goephys. Res. Atmos.* **2013**, *118*, 12497–12507. [CrossRef]
22. Wilcox, B.; Mitchell, K.; Schwandner, F.; Lopes, R. Defending Human Civilization from Large Volcanic Eruptions. 2015. Available online: https://scienceandtechnology.jpl.nasa.gov/sites/default/files/documents/DefendingCivilizationFromSupervolcanos20151015.pdf (accessed on 10 October 2022).
23. Fischer, T.P.; Chiodini, G. Volcanic, Magmatic, and Hydrothermal Gases. In *The Encyclopedia of Volcanoes*; Academic Press: Cambridge, MA, USA, 2015; pp. 779–797.
24. Black, B.A.; Neely, R.R.; Lamarque, J.-F.; Elkins-Tanton, L.T.; Kiehl, J.T.; Shields, C.A.; Mills, M.J.; Bardeen, C. Systemic swings in end-Permian climate from Siberian Traps carbon and sulfur outgassing. *Nat. Geosci.* **2018**, *11*, 949–954. [CrossRef]

25. Aiuppa, A.; Fischer, T.P.; Plank, T.; Bani, P. Volcanic gas emissions and secondary aerosol formation. *Geochem. Geophys. Geosyst.* **2017**, *18*, 3337–3365.
26. Newnham, R.M.; Dirks, K.N.; Samaranayake, D. An investigation into long-distance health impacts of the 1996 eruption of Mt Ruapehu, New Zealand. *Atmos. Environ.* **2010**, *44*, 1568–1578. [CrossRef]
27. Nicole, W. Clear and Present Dangers: The Multiple Health Hazards of Volcanic Eruptions. *Environ. Health Perspect.* **2022**, *130*, 22001. [CrossRef]
28. Stewart, C.; Damby, D.E.; Horwell, C.J.; Elias, T.; Ilyinskaya, E.; Tomašek, I.; Longo, B.M.; Schmidt, A.; Carlsen, H.K.; Mason, E.; et al. Volcanic air pollution and human health: Recent advances and future directions. *Bull. Volcanol.* **2021**, *84*, 11. [CrossRef]
29. Trisnawati, I.; Budiono, E.; Sumardi; Setiadi, A. Traumatic Inhalation due to Merapi Volcanic Ash. *Acta Medica Indones.* **2015**, *47*, 238–243.
30. Gui, K.; Che, H.; Tian, L.; Wang, Y.; Shi, C.; Yao, W.; Liang, Y.; Li, L.; Zheng, Y.; Zhang, L.; et al. Columnar optical, microphysical and radiative properties of the 2022 Hunga Tonga volcanic ash plumes. *Sci. Bull.* **2022**, *67*, 2013–2021. [CrossRef]
31. Teller, E.; Wood, L.; Hoover Institution; Hyde, R. Global warming and ice ages. In *The Carbon Dioxide Dilemma*; 22. UCRL-JC 135414; Lawrence Livermore National Laboratory: Livermore, CA, USA, 1997.
32. Teller, E.; Hyde, R.; Wood, L. *Active Climate Stabilization: Practical Physics-Based Approaches to Prevention of Climate Change*; Lawrence Livermore National Laboratory: Livermore, CA, USA, 2002.
33. National Academies of Sciences, Engineering, and Medicine. *Reflecting Sunlight: Recommendations for Solar Geoengineering Research and Research Governance*; The National Academies Press: Washington, DC, USA, 2021. [CrossRef]
34. Haywood, J.; Tilmes, S.; Keutsch, F.; Niemeier, U.; Schmidt, A.; Visioni, D.; Yu, P. *Stratospheric Aerosol Injection and its Potential Effect on the Stratospheric Ozone Layer, Chapter 6 in Scientific Assessment of Ozone Depletion: 2022*, GAW Report No. 278; WMO: Geneva, Switzerland, 2022; 509p.
35. Parker, A.; Horton, J.B.; Keith, D.W. Stopping Solar Geoengineering Through Technical Means: A Preliminary Assessment of Counter-Geoengineering. *Earth's Future* **2018**, *6*, 1058–1065. [CrossRef]
36. Denkenberger, D.C.; Blair, R.W. Interventions that may prevent or mollify large volcanic eruptions. *Futures* **2018**, *102*, 51–62. [CrossRef]
37. Shaffer, G. Long time management of fossil fuel resources to limit global warming and avoid ice age onsets. *Geophys. Res. Lett.* **2009**, *36*, L03704. [CrossRef]
38. Fuglestvedt, J.S.; Samset, B.H.; Shine, K.P. Counteracting the climate effects of volcanic eruptions using short-lived greenhouse gases. *Geophys. Res. Lett.* **2014**, *41*, 8627–8635. [CrossRef]
39. Newhall, C.; Self, S.; Robock, A. Anticipating future Volcanic Explosivity Index (VEI) 7 eruptions and their chilling impacts. *Geosphere* **2018**, *14*, 572–603. [CrossRef]
40. Hasselmann, K. Stochastic climate models Part I. Theory. *Tellus* **1976**, *28*, 473–485.
41. The Nobel Committee for Physics. *Scientific Background on the Nobel Prize in Physics 2021: For Groundbreaking Contributions to Our Understanding of Complex Physical Systems*; The Royal Swedish Academy of Sciences: Stockholm, Sweden, 2021.
42. Ramanathan, V.; Xu, Y. The Copenhagen Accord for limiting global warming: Criteria, constraints, and available avenues. *Proc. Natl. Acad. Sci. USA* **2010**, *107*, 8055–8062. [CrossRef]
43. Hu, A.; Xu, Y.; Tebaldi, C.; Washington, W.M.; Ramanathan, V. Mitigation of short-lived climate pollutants slows sea-level rise. *Nat. Clim. Chang.* **2013**, *3*, 730–734. [CrossRef]
44. IPCC. *Climate Change 2014: Synthesis Report. Contribution of Working Groups I, II and III to the Fifth Assessment Report of the Intergovernmental Panel on Climate Change*; Core Writing Team, Pachauri, R.K., Meyer, L.A., Eds.; IPCC: Geneva, Switzerland, 2014; 151p.
45. Hodnebrog, Ø.; Aamaas, B.; Fuglestvedt, J.S.; Marston, G.; Myhre, G.; Nielsen, C.J.; Sandstad, M.; Shine, K.P.; Wallington, T.J. Updated Global Warming Potentials and Radiative Efficiencies of Halocarbons and Other Weak Atmospheric Absorbers. *Rev. Geophys.* **2020**, *58*, e2019RG000691. [CrossRef]
46. Velders, G.J.M.; Fahey, D.W.; Daniel, J.S.; Andersen, S.O.; McFarland, M. Future atmospheric abundances and climate forcings from scenarios of global and regional hydrofluorocarbon (HFC) emissions. *Atmos. Environ.* **2015**, *123*, 200–209. [CrossRef]
47. Velders, G.J.M.; Fahey, D.W.; Daniel, J.S.; McFarland, M.; Andersen, S.O. The large contribution of projected HFC emissions to future climate forcing. *Proc. Natl. Acad. Sci. USA* **2009**, *106*, 10949–10954. [CrossRef]
48. Xu, Y.; Zaelke, D.; Velders, G.J.M.; Ramanathan, V. The role of HFCs in mitigating 21st century climate change. *Atmos. Chem. Phys.* **2013**, *13*, 6083–6089. [CrossRef]
49. IEA. *Natural Gas Information: Overview*; IEA: Paris, France, 2021; Available online: https://www.iea.org/reports/natural-gas-information-overview (accessed on 10 October 2022).
50. United Nations Environment Programme and International Energy Agency. *Cooling Emissions and Policy Synthesis Report: Benefits of Cooling Efficiency and the Kigali Amendment*; UNEP: Nairobi, Kenya; IEA: Paris, France, 2020.
51. Stenchikov, G.L.; Kirchner, I.; Robock, A.; Graf, H.; Antuña, J.C.; Grainger, R.G.; Lambert, A.; Thomason, L. Radiative forcing from the 1991 Mount Pinatubo volcanic eruption. *J. Geophys. Res. Atmos.* **1998**, *103*, 13837–13857. [CrossRef]
52. Ramachandran, S.; Ramaswamy, V.; Stenchikov, G.L.; Robock, A. Radiative impact of the Mount Pinatubo volcanic eruption: Lower stratospheric response. *J. Geophys. Res. Atmos.* **2000**, *105*, 24409–24429. [CrossRef]

53. Soden, B.J. Global Cooling After the Eruption of Mount Pinatubo: A Test of Climate Feedback by Water Vapor. *Science* **2002**, *296*, 727–730. [CrossRef] [PubMed]
54. Bender, F.A.-M.; Ekman, A.M.L.; Rodhe, H. Response to the eruption of Mount Pinatubo in relation to climate sensitivity in the CMIP3 models. *Clim. Dyn.* **2010**, *35*, 875–886. [CrossRef]
55. Timmreck, C.; Graf, H.; Lorenz, S.J.; Niemeier, U.; Zanchettin, D.; Matei, D.; Jungclaus, J.H.; Crowley, T.J. Aerosol size confines climate response to volcanic super-eruptions. *Geophys. Res. Lett.* **2010**, *37*, L24705. [CrossRef]
56. Lane, C.S.; Brauer, A.; Blockley, S.P.E.; Dulski, P. Volcanic ash reveals time-transgressive abrupt climate change during the Younger Dryas. *Geology* **2013**, *41*, 1251–1254. [CrossRef]
57. Smith, E.I.; Jacobs, Z.; Johnsen, R.; Ren, M.; Fisher, E.C.; Oestmo, S.; Wilkins, J.; Harris, J.A.; Karkanas, P.; Fitch, S.; et al. Humans thrived in South Africa through the Toba eruption about 74,000 years ago. *Nature* **2018**, *555*, 511–515. [CrossRef]
58. Chen, J.; Cui, H.; Xu, Y.; Ge, Q. An Investigation of Parameter Sensitivity of Minimum Complexity Earth Simulator. *Atmosphere* **2020**, *11*, 95. [CrossRef]
59. Chen, J.; Cui, H.; Xu, Y.; Ge, Q. Long-term temperature and sea-level rise stabilization before and beyond 2100: Estimating the additional climate mitigation contribution from China's recent 2060 carbon neutrality pledge. *Environ. Res. Lett.* **2021**, *16*, 074032. [CrossRef]
60. Hanna, R.; Abdulla, A.; Xu, Y.; Victor, D. Emergency deployment of direct air capture as a response to the climate crisis. *Nat. Commun.* **2021**, *12*, 368. [CrossRef]
61. Self, S.; Blake, S. Consequences of Explosive Supereruptions. *Elements* **2008**, *4*, 41–46. [CrossRef]
62. Archer, D.; Eby, M.; Brovkin, V.; Ridgwell, A.; Cao, L.; Mikolajewicz, U.; Caldeira, K.; Matsumoto, K.; Munhoven, G.; Montenegro, A.; et al. Atmospheric Lifetime of Fossil Fuel Carbon Dioxide. *Annu. Rev. Earth Planet. Sci.* **2009**, *37*, 117–134. [CrossRef]
63. Löffler, M.; Brinkop, S.; Jöckel, P. Impact of major volcanic eruptions on stratospheric water vapour. *Atmos. Chem. Phys.* **2016**, *16*, 6547–6562. [CrossRef]
64. Jenkins, S.; Smith, C.; Allen, M.; Grainger, R. Tonga eruption increases chance of temporary surface temperature anomaly above 1.5 °C. *Nat. Clim. Chang.* **2023**, *13*, 127–129. [CrossRef]
65. Guzewich, S.D.; Oman, L.D.; Richardson, J.A.; Whelley, P.L.; Bastelberger, S.T.; Young, K.E.; Bleacher, J.E.; Fauchez, T.J.; Kopparapu, R.K. Volcanic Climate Warming Through Radiative and Dynamical Feedbacks of SO_2 Emissions. *Geophys. Res. Lett.* **2022**, *49*, e2021GL096612. [CrossRef]
66. Jaccaud, M.; Faron, R.; Devilliers, D.; Romano, R.; Riedel, S.; Pernice, H. Fluorine. In *Ullmann's Encyclopedia of Industrial Chemistry*; Wiley: Hoboken, NJ, USA, 2020; pp. 1–19. [CrossRef]
67. Hayes, T.S.; Miller, M.M.; Orris, G.J.; Piatak, N.M. Fluorine. In *U.S. Geological Survey Professional Paper*; Professional Paper 1802–G; U.S. Geological Survey: Reston, VA, USA, 2017.
68. U.S. Geological Survey. *Mineral Commodity Summaries 2020*; U.S. Geological Survey: Reston, VA, USA, 2020. [CrossRef]
69. Tressaud, A. *Fluorine*; Academic Press: Cambridge, MA, USA, 2018.
70. Wilson, C.J.N.; Cooper, G.F.; Chamberlain, K.J.; Barker, S.J.; Myers, M.L.; Illsley-Kemp, F.; Farrell, J. No single model for supersized eruptions and their magma bodies. *Nat. Rev. Earth Environ.* **2021**, *2*, 610–627. [CrossRef]
71. Morton, M.C.; Don't Call It a Supervolcano. Eos. 2021. Available online: https://eos.org/features/dont-call-it-a-supervolcano (accessed on 10 October 2022).
72. Cao, L.; Duan, L.; Bala, G.; Caldeira, K. Simultaneous stabilization of global temperature and precipitation through cocktail geoengineering. *Geophys. Res. Lett.* **2017**, *44*, 7429–7437. [CrossRef]
73. Brasseur, G.; Orlando, J.J.; Tyndall, G.S.; National Center For Atmospheric Research. *U.S. Atmospheric Chemistry and Global Change*; Oxford University Press: Oxford, UK, 1999.
74. Li, M.; Karu, E.; Brenninkmeijer, C.; Fischer, H.; Lelieveld, J.; Williams, J. Tropospheric OH and stratospheric OH and Cl concentrations determined from CH_4, CH_3Cl, and SF_6 measurements. *NPJ Clim. Atmos. Sci.* **2018**, *1*, 29. [CrossRef]
75. Stevenson, D.S.; Johnson, C.E.; Highwood, E.J.; Gauci, V.; Collins, W.J.; Derwent, R.G. Atmospheric impact of the 1783–1784 Laki eruption: Part I Chemistry modelling. *Atmos. Chem. Phys.* **2003**, *3*, 487–507. [CrossRef]
76. Tilmes, S.; Richter, J.H.; Mills, M.J.; Kravitz, B.; MacMartin, D.G.; Vitt, F.; Tribbia, J.J.; Lamarque, J. Sensitivity of Aerosol Distribution and Climate Response to Stratospheric SO_2 Injection Locations. *J. Geophys. Res. Atmos.* **2017**, *122*, 12591–12615. [CrossRef]
77. Tilmes, S.; Richter, J.H.; Kravitz, B.; MacMartin, D.G.; Mills, M.J.; Simpson, I.R.; Glanville, A.S.; Fasullo, J.T.; Phillips, A.S.; Lamarque, J.-F.; et al. CESM1(WACCM) Stratospheric Aerosol Geoengineering Large Ensemble Project. *Bull. Am. Meteorol. Soc.* **2018**, *99*, 2361–2371. [CrossRef]
78. Visioni, D.; MacMartin, D.G.; Kravitz, B.; Tilmes, S.; Mills, M.J.; Richter, J.H.; Boudreau, M.P. Seasonal Injection Strategies for Stratospheric Aerosol Geoengineering. *Geophys. Res. Lett.* **2019**, *46*, 7790–7799. [CrossRef]
79. Xu, Y.; Lin, L.; Tilmes, S.; Dagon, K.; Xia, L.; Diao, C.; Cheng, W.; Wang, Z.; Simpson, I.; Burnell, L. Climate engineering to mitigate the projected 21st-century terrestrial drying of the Americas: A direct comparison of carbon capture and sulfur injection. *Earth Syst. Dyn.* **2020**, *11*, 673–695. [CrossRef]

80. North, G.R.; Kim, K.-Y. *Energy Balance Climate Models*; Weinheim Wiley-Vch: Weinheim, Germany, 2017.
81. Biermann, F.; Oomen, J.; Gupta, A.; Ali, S.H.; Conca, K.; Hajer, M.A.; Kashwan, P.; Kotzé, L.J.; Leach, M.; Messner, D.; et al. Solar geoengineering: The case for an international non-use agreement. *WIREs Clim. Chang.* **2022**, *13*, e754. [CrossRef]